


RESEARCH ARTICLE

Along-strike variation of fault slip rate of a transform plate boundary in Tierra del Fuego (South Patagonia)

Riccardo Vassallo¹ | Joseph Martinod¹ | Sandrine Roy¹  | Christian Sue¹ | Laurent Astrade²

¹ISTerre, Université Savoie Mont Blanc, Université Grenoble Alpes, CNRS, IRD, Université G. Eiffel, Le Bourget du Lac, France

²Edytem, Université Savoie Mont Blanc, Le Bourget du Lac, France

Correspondence

Riccardo Vassallo, ISTerre, Université Savoie Mont Blanc, Université Grenoble Alpes, CNRS, IRD, Université G. Eiffel, Le Bourget du Lac, France.
Email: riccardo.vassallo@univ-smb.fr

Funding information

Institut national des sciences de l'Univers; Centre National de la Recherche Scientifique; Institut de Recherche pour le Développement

Abstract

The Magallanes–Fagnano Fault is an active strike-slip structure accommodating the relative displacement between South America and the Scotia Plate. The Chilean portion of the fault is poorly studied because most of it runs below the sea level in the Strait of Magellan. Our tectonic geomorphological study is focused on a rare onshore fault section, along which streams horizontally deflected by hundreds of metres since the last main deglaciation are compatible with a dominant left-lateral fault kinematics and yield a slip rate of 15.7 ± 2.4 mm/year. This rate is between 2 and 3 times higher than the one estimated on the Argentinian portion of the fault over the same period. This spatial variation may be due to both glacial unloading on the fault zone and/or structural factors. These results point out the need to study strike-slip faults on several portions to unravel behaviour changes related to internal or external forcing.

KEYWORDS

ice loading, slip rate variation, South America, strike-slip fault, tectonic geomorphology

1 | INTRODUCTION

Large strike-slip fault systems, characterized by structures several 1000 km long, involve large and continuous seismogenic zones with high potential for triggering destructive earthquakes. The 2023 seismic events of Mw 7.8 and 7.5 occurred in few hours along the East Anatolian Fault in Turkey and Syria, causing tens of thousands of victims, are the latest examples illustrating the dangerousness of this type of tectonic structures. The frequency of these earthquakes depends on the fault slip rate, mainly controlled by tectonic loading. However, due to second-order processes we discuss below, slip rates may vary both along strike and in time. Few faults have been studied from this perspective, and the causes of these variations are often poorly understood.

Along-strike-slip rate gradients have been observed and generally attributed to endogenous parameters such as the orientation

changes in relation to regional stress, the partitioning of deformation or the lithospheric thickness (Chevalier et al., 2016; Kirby et al., 2007; Liu et al., 2020; Matmon et al., 2006). Millennial-scale temporal variations have been even more rarely reported and have been mainly ascribed to regional tectonic rate changes or fault strength alterations (Bennett et al., 2004; Dolan et al., 2016, 2024; Gold & Cowgill, 2011; Ninis et al., 2013; Zinke et al., 2021). No case studies deal with the impact of glacier dynamics on transform fault slip rate variability, though theoretically significant. Indeed, mechanical models show that flexure of the lithosphere may cause an increase in compressive tangential stress in the seismogenic crust, which may delay the occurrence of earthquakes (Hampel et al., 2009; Steffen & Steffen, 2021). The Magallanes–Fagnano Fault (MFF), crossing a region characterized by major Quaternary glaciation–deglaciation phases, offers excellent conditions to better understand the effects of such tectonic–climatic interactions.

This is an open access article under the terms of the [Creative Commons Attribution-NonCommercial-NoDerivs](https://creativecommons.org/licenses/by-nc-nd/4.0/) License, which permits use and distribution in any medium, provided the original work is properly cited, the use is non-commercial and no modifications or adaptations are made.

© 2024 The Authors. *Terra Nova* published by John Wiley & Sons Ltd.

2 | GEOLOGICAL SETTING

The Strait of Magellan, at the southern tip of America, has been shaped by the interaction between strike-slip faulting and glacier erosion during Quaternary. The MFF is a major left-lateral transform fault system that separates the austral segment of South America from the Scotia Plate (Ghiglione, 2002; Klepeis, 1994; Lodolo et al., 2003; Tassone et al., 2005, 2008; Torres Carbonell et al., 2008; Winslow, 1982). The onset of strike-slip faulting in Tierra del Fuego along the MFF probably occurred during the late Miocene (Torres Carbonell et al., 2014). This transform plate boundary is mapped from the Pacific entrance of the Strait of Magellan to the Scotia subduction zone in the Atlantic Ocean (Figure 1). Most of this fault system is offshore, Tierra del Fuego owing its largest onshore section. This fault already triggered three strong earthquakes in barely two centuries of historical record (Costa et al., 2006; Febrer et al., 2000; Jaschek et al., 1982; Pelayo & Wiens, 1989). The latest major seismic sequence is extraordinarily similar to the 2023 Eastern Anatolian Fault one, with the occurrence of a Mw 7.8 followed by a Mw 7.5 in less than 1 day in December 1949, although we do not know whether they occurred on the same fault, or on a different one, as in Turkey. Another Mw 7–7.5 shook the region in 1879, at the beginning of the settlements in Ushuaia and Punta Arenas (Lomnitz, 1970).

Tierra del Fuego was largely covered by ice during the last glacial period (Figure 1). Observations of the trimline at ~700ma.s.l. in the area between the Almirantazgo Sound and Lake Fagnano suggest a maximum ice thickness of approximately 1 km. Fault morphology was reset by glacier erosion, and tectonic deformation has been recorded in the landforms during post-glacial period. Fault slip rates were determined along its Argentinian portion at the present and at the millennial time-scale, both estimates yielding a sinistral velocity of 6–7 mm/year (Mendoza et al., 2015; Roy et al., 2020; Sandoval & de Pascale, 2020; Smalley et al., 2003). On the other hand, due to the difficult accessibility and the position of large part of the fault trace below the sea, fault slip rates for the Chilean portion of the fault have not been quantified. Between the Strait of Magellan and Fagnano Lake, the fault trace is often confounded with bedrock inherited structures along the steep mountain slopes with neither suitable nor datable markers that could be used to get a robust slip rate. The only obvious onshore active fault segment in Chile is limited to a 10-km-wide advance of land into the sea: the Ainsworth Peninsula.

3 | THE AINSWORTH PENINSULA FAULT ZONE

During last glacial period, the fjords of the Strait of Magellan were largely carved by glacier action. The MFF runs mostly in the middle of the main fjord, but it is clearly visible on the Ainsworth Peninsula, the most prominent land advance in the southern part of this area. This peninsula is characterized in its NE portion by metamorphic Middle/Upper Jurassic volcanoclastic bedrock belonging

Significance Statement

Our study focuses on the active tectonics of the Magellan–Fagnano Fault (South Patagonia), in the Chilean part of the transform plate boundary for which no data of Quaternary activity are available up to date. Using tectonic geomorphology and geochronology, we determined post-glacial deformation stages and fault slip rate along this section, as already done for the Argentinian portion of the fault (Roy et al., 2020). We highlight an along-strike-slip rate variation over the last ~16 ka. We argue it may be partially timely related due to ice unloading above the fault zone during last glaciation period.

to the Tobifera Formation (Pankhurst, 2000; Thomas, 1949) and polished by glacier erosion, while its SW portion is covered by soft sediments mainly constituted by till deposits (Figure 2a). In this latter part, topography has a constant slope of 6° to the NE, locally perturbed by flatter areas elongated parallelly to the axis of the main valley that may be interpreted as kame terraces (Figure 2). Here, a coloured patchwork of peat covering the ground is locally interspersed by lines of tree vegetation growing along the drainage network. This network is constituted by temporary streams of few metres deep, most of which are straight and parallel to the main slope until they intersect a perpendicular lineament, associated with a few metres high scarp, corresponding to the fault trace. This regular pattern, due to a low degree of hierarchization of the drainage network, is highly perturbed crossing the fault zone. Some streams are laterally deflected by several tens or hundreds of metres with bayonet geometries, whose most spectacular manifestation is a continuous sigmoidal shape showing a deflection of 274 ± 40 m (Figure 2b,c). Other streams stop abruptly at the toes of the scarp in a locally flat swampy zone. Symmetrically, downstream of the fault zone we notice the presence of some beheaded channels. All these geomorphic features are compatible with cumulative deformation along a unique fault segment characterized by dominant left-lateral strike-slip.

A hand-made trench across the scarp revealed both the shallow stratigraphy of the deposits and the deformation affecting them (Figure 3). Till and colluvium lie over lacustrine sediments, from which they are separated by an erosive contact. The apparent dip of silty–sandy lacustrine layers dated at 42–51 ka (Table 1) varies from 10° SW to 40° NE across the scarp, indicating a gentle folding. Several ruptures dipping strongly to the SW affect both lacustrine and glacial deposits with small apparent reverse and normal offsets. These observations, which attest to the presence of localized surface deformation along the fault, are typical of positive flower structure consistent with dominant strike-slip kinematics. They also show that the last glaciation significantly eroded the unconsolidated sediments situated in the area, leading to a rejuvenation of the landscape.

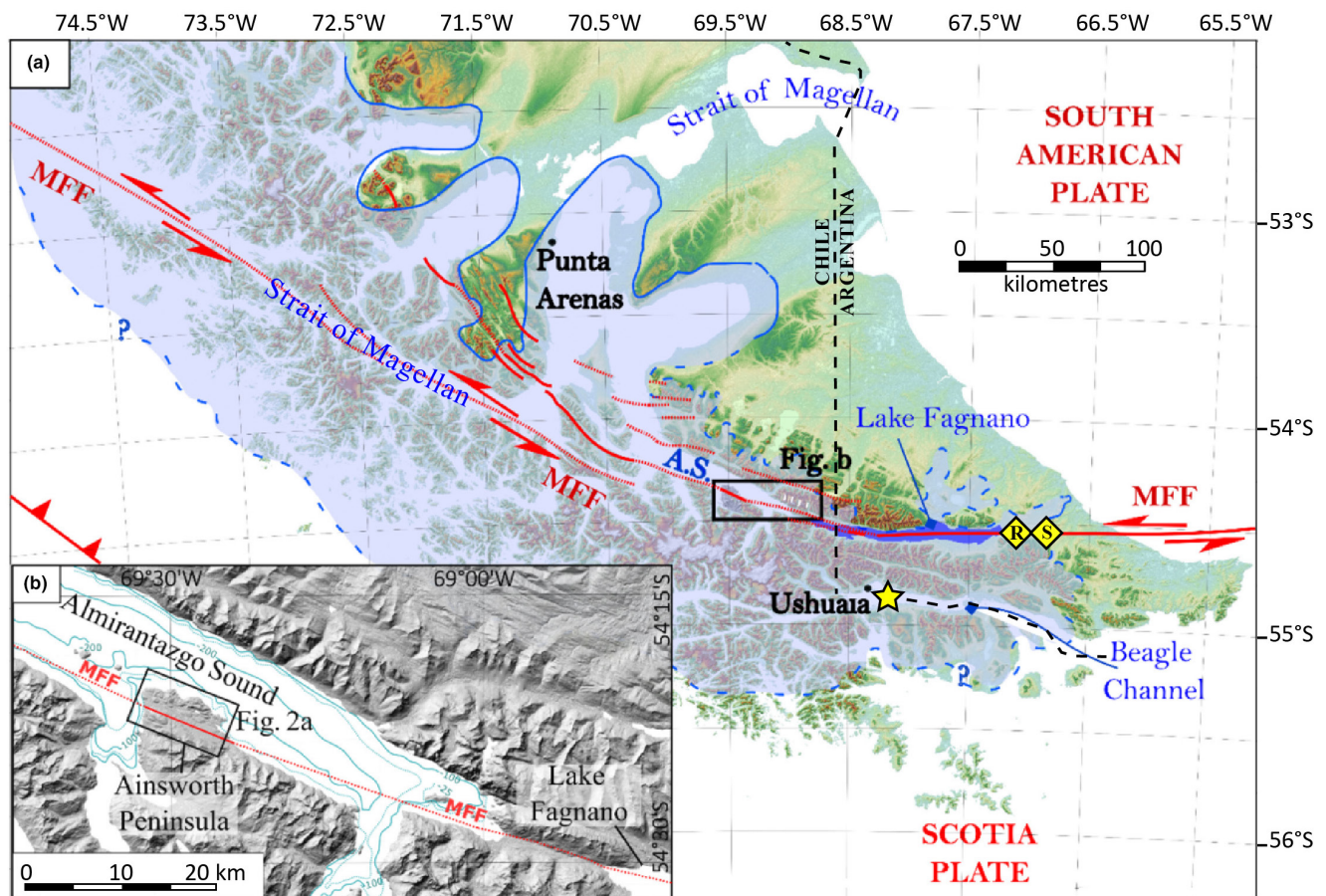


FIGURE 1 (a) Tectonic map of the Magallanes–Fagnano Fault (MFF) zone with Last Glacial Maximum (LGM) ice extension in the Southern Andes. The red lines indicate the recognized MFF fault sections, and the dashed red lines indicate the MFF interpolated traces (Betka et al., 2016; Cunningham, 1993; Esteban et al., 2014; Fernández et al., 2017; Klepeis, 1994; Klepeis & Austin, 1997; Lodolo et al., 2003; Onorato et al., 2021; Perucca et al., 2016; Roy et al., 2020; Sandoval & de Pascale, 2020; Smalley et al., 2003; Winslow, 1982). Yellow diamonds indicate the slip rate sites of Roy et al. (2020) (R) and Sandoval and De Pascale (2020) (S). Yellow star indicates the offshore study area of Bran et al. (2023). The base map is the shaded DEM SRTM ALOS World 3D-30m (©JAXA). The blue line shows the LGM extensions (Bentley et al., 2005; Boyd et al., 2008; Clapperton et al., 1995; Coronato et al., 2004, 2009; Davies et al., 2020; Fernández et al., 2017; Hall et al., 2019; McCulloch et al., 2005; Rabassa et al., 2000). The blue dashed line is the poorly constrained extension. A.S. stands for Almirantazgo Sound. (b) Map of the Almirantazgo Sound showing location of the Ainsworth Peninsula study site and the MFF trace. Bathymetry of Almirantazgo Sound with a 50-m contour interval is the Esri, GEBCO, NOAA (2014) grid.

4 | BACK-SLIP RESTORATION

Back-slip restoration at the scale of the Ainsworth Peninsula is based on the realignment of streams uphill and downhill the fault scarp going back in time. Considering nine principal streams crossing the fault, the realignment of several of them at a tectonic stage determines the simultaneous setting up of a localized drainage system (Figure 4). Compared to the measurement of distinct piercing points, this technique being based on multiple geometrical constraints results in more robust offset restoration with improved measurement accuracy. Each stream generation, triggered by particular climatic/erosional conditions, records the cumulative strike-slip deformation by incremental lateral displacement along the fault zone. The slight uplift of the upstream block determines the absence of major counterscarps along the fault that could promote non-tectonic deflections.

We put in evidence two well-defined back-slip stages. Stage 1 is determined by the realignment of 5 streams at 120 ± 10 m of back-slip restoration. Stage 2 is determined by the realignment of 4 streams at 260 ± 20 m. This stage corresponds to the oldest possible configuration. Since displacements in the central part of the fault zone are larger than the spacing between streams, two of them situated downstream of the fault have been successively fed by two different channels during stages 1 and 2.

5 | DATING THE CUMULATIVE DEFORMATION

The benefit of using a poorly hierarchized drainage network for back-slip restoration is the availability, in a relatively small area, of several suitable markers for an accurate reconstruction of past geometries.

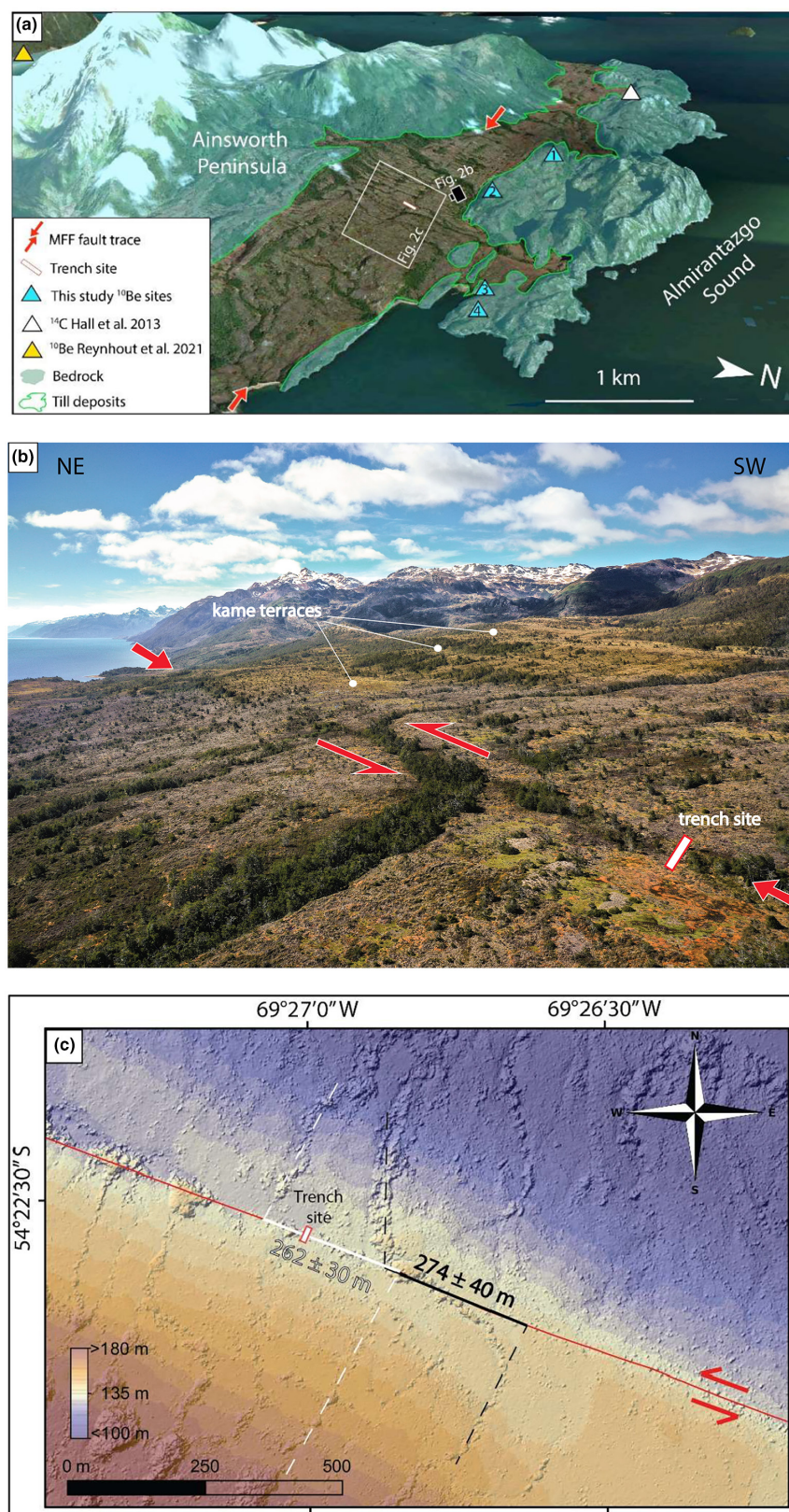


FIGURE 2 (a) Geological map of the Ainsworth Peninsula. The blue triangles 1–4 refer to ^{10}Be samples T1 to T4 with ages available in Table 1. The base map is satellite Bing™ Map with 2× exaggerated relief. (b) Aerial view of the left-lateral stream deflection by the Magallanes–Fagnano Fault, indicated by red arrows; other views of the fault zone are available in Supplemental File S1. (c) Digital Surface Model of a portion of the fault zone obtained from Pleiades images (1 m resolution). Streams appear as apparent positive relief associated with top of trees growing inside them. Note the slight obliquity of the main stream with respect to the fault scarp direction, excluding possible non-tectonic deflection linked to fault topographic barrier.

The disadvantage is that we cannot directly date the setting of these markers. We thus need to date the genesis of the landforms successively incised by streams assuming that these depositional/erosional events are almost synchronous. In this context, we supposed that the onset of the drainage network started with the retreat of the glaciers

from the Ainsworth Peninsula. Dating of the glacial retreat therefore yields the best estimate for the age of the oldest back-slip stage.

We collected 4 samples of polished bedrock for ^{10}Be exposure dating (Figure 2a). Considering no bedrock denudation since deglaciation, we obtained 3 similar minimal exposure ages within analytical

FIGURE 3 (a) Photomosaic of the trench western wall (−54.375606, −69.449923); detailed views are available in Supplemental File S1. (b) Interpretative logs and sample locations. Details on ^{14}C samples are given in Table 1 (all the ages are calibrated, except sample C2). (c) Interpreted fault zone geometry at depth.

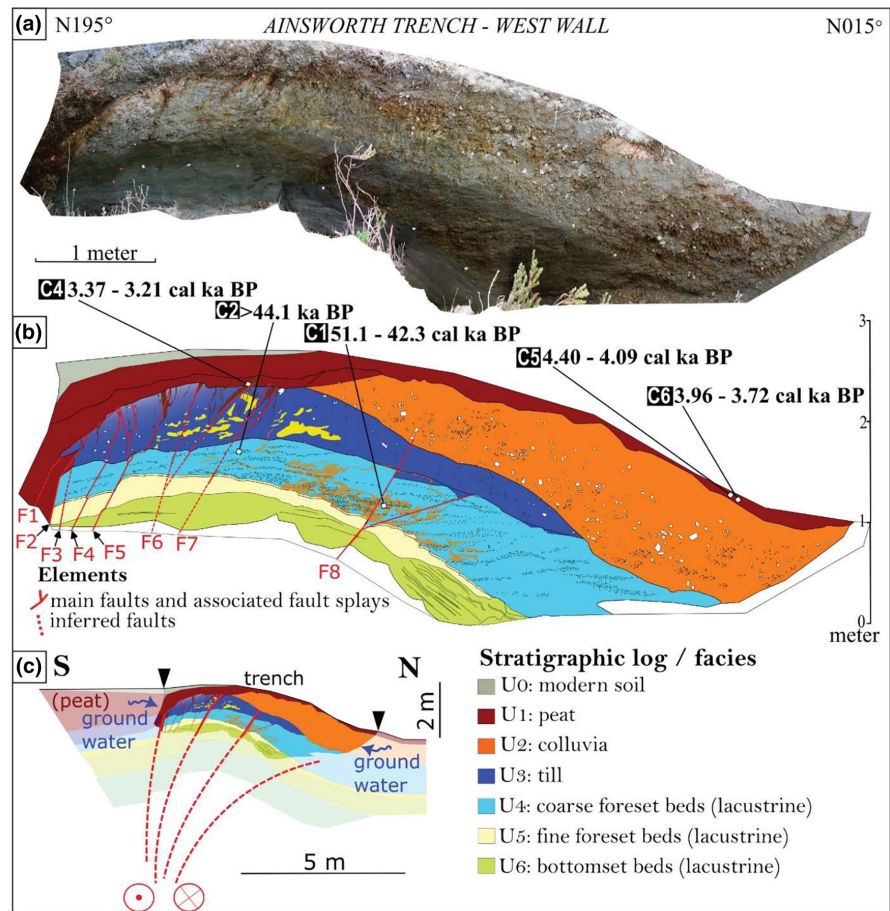


TABLE 1 Mass spectrometry measurements of radiocarbon samples.

Sample	Lat°/long°	N°SaCa	IGSN	Nature	Unit	Mass spectrometry measurements (ages and errors in years BP)					Calibrated ages (cal years BP)	
						mg C	Delta ^{13}C	pMC	^{14}C age	Err	From	To
C1	54.375606°S, 69.449923°W	60,318	IEROY000T	Charcoal	U4	1.66	−22.1	0.567 ± 0.141	41,600	2000	51,139	42,276
C2	54.375606°S, 69.449923°W	61,164	IEROY000U	Charcoal	U4	0.96	−18.3	<0.41 ^a	>44,100	NA	NA	NA
C4	54.375606°S, 69.449923°W	60,319	IEROY000V	Charcoal	U1	0.89	−33.6	68.168 ± 0.232	3080	30	3370	3212
C5	54.375606°S, 69.449923°W	60,320	IEROY000W	Charcoal	U1	1.29	−24.3	62.078 ± 0.209	3830	30	4402	4097
C6	54.375606°S, 69.449923°W	60,321	IEROY000X	Charcoal	U1	1.35	−26.2	64.336 ± 0.213	3545	30	3959	3718

Note: The ages are calibrated using OxCal version 4.4 (Ramsey, 2009, 2017) with atmospheric curve SHCal 20 (Hogg et al., 2013). Note that the measurements were made at LMC14, CEA, Saclay, France, using the Artemis accelerator mass spectrometry (AMS) facility following preparation protocols (Dumoulin et al., 2017; Moreau et al., 2020).

Abbreviations: Delta ^{13}C , per cent of isotope ^{13}C ; IGSN, International Geo Sample Number; mg C, amount of carbon in mg; pMC, per cent modern carbon.

^aApparent age close to background: $1\sigma < \text{measured sample activity} < 2\sigma$. Error on ^{14}C age and calibration not applicable (NA).

errors at 16 ± 2 ka, with an older one at 21.7 ± 3.2 ka (Table 2). Our ages at ~16 ka are compatible with the dating in the Ainsworth Peninsula based on ^{14}C on organic rests in cores from peatbog above glacial sediments ranging from 17.1 to 15.5 cal ka BP (Hall et al., 2013) and on ^{10}Be on the frontal moraine at the mouth of the fjord that borders the Ainsworth Peninsula to the north-west at ~16.5 ka

(Reynhout et al., 2021) (Figure 2a). They are also consistent with the whole deglaciation history in the Strait evidencing a rapid ice sheet shrinking of piedmont glaciers at ~17.5 ka (Davies et al., 2020; McCulloch et al., 2005). Considering both our dates and the previous contributions, we may set the deglaciation of the Ainsworth Peninsula at 16.5 ± 1 ka.

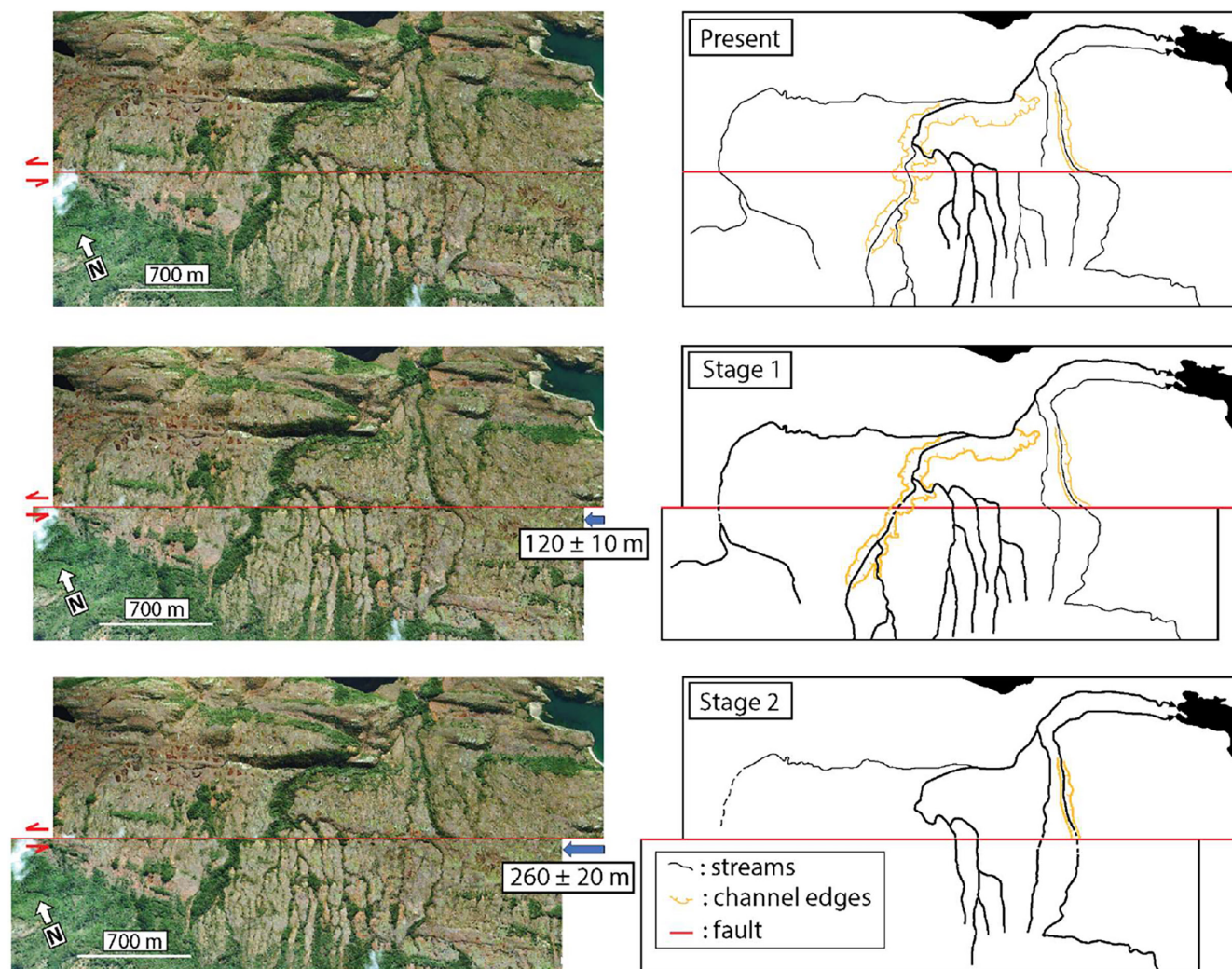


FIGURE 4 Back-slip restoration in 2 stages (120 ± 10 m and 260 ± 20 m) using the drainage network deflected by the MFF (Bing™ satellite image). At each stage, streams aligned on both sides of the fault (in bold) are newly formed and their final deflection corresponds to the following cumulative strike-slip deformation.

TABLE 2 ^{10}Be measurements.

Sample	Lat°/long°	Altitude (m.a.s.l.)	Nature	^{10}Be (at/g)	Error ^{10}Be (at/g)	Production rate (at/g/year)	Error on production rate (at/g/year)	Shielding	Age (years)	Error on age (years)
T1	54.36083°S, 69.47073°W	121	Polished bedrock	88,488	7266	5.25	0.45	0.998799	16,715	2817
T2	54.36493°S, 69.45719°W	74	Polished bedrock	77,489	6016	5.01	0.43	0.998799	15,685	2547
T3	54.36978°S, 69.43087°W	40	Polished bedrock	74,765	2698	4.84	0.42	0.999604	15,613	1912
T4	54.36924°S, 69.42814°W	23	Polished bedrock	1,01,718	6646	4.75	0.41	0.999161	21,697	3721

Note: All measurements were made at Laboratoire National des Nucléides Cosmogéniques LN2C (Cerege, Aix-en-Provence, France) using the accelerator 5 MV ASTER and following the procedure of Braucher et al. (2015). Errors on ^{10}Be concentrations include measurement (number of count), standard (certification), average standard measurements (machine) and systematic error (machine external error 0.5%, Arnold et al., 2010). The production rates have been calculated following Stone (2000) using modified scaling function from Lal (1991). The topographic shielding calculator used in this study is [Stoneage.ice-d.org](https://www.ice.d.org) version 2.

6 | DISCUSSION AND CONCLUSIONS

We determined two back-slip drainage stages, which we interpret as climatic/erosional events associated with an enhanced regressive erosion of the streams across the fault zone. We propose that the pristine drainage network corresponds to the oldest back-slip stage found at the Ainsworth Peninsula, after landscape resetting by glaciers. These streams therefore recorded the cumulative tectonic deformation along the MFF during the whole post-glacial period. The youngest back-slip stage may correspond to a successive climatic event, associated with a second generation of first-order streams.

The geomorphic fault slip rate obtained using the oldest deformation stage (260 ± 20 m) and the age of the glacier retreat (16.5 ± 1 ka) is 15.7 ± 2.4 mm/year. This millennial rate is the only one available for the portion of the MFF in the Strait of Magellan, since the sparse GNSS network in the Chilean region of the fault is unsuited to study tectonic activity. However, this slip rate is between 2 and 3 times higher than the rate estimated on the Argentinian portion of the fault at 6–7 mm/year (Roy et al., 2020; Sandoval & de Pascale, 2020). This significant difference may be ascribed to several non-exclusive possibilities:

1. Part of the deformation in the eastern region may be distributed over several faults. GNSS data in Argentinian Tierra del Fuego and morphological analysis around Fagnano Lake tend to exclude the existence of another important structure on the island. Nevertheless, a recent study shows the presence of Holocene strike-slip deformation in the Beagle Channel (Bran et al., 2023; see Figure 1), which could be a good candidate for hosting significant offshore faulting sub-parallel to the main branch of MFF.
2. The bend of the MFF of 20° between the Strait of Magellan and Fagnano Lake may reduce the strike-slip component to the east in favour of an enhanced transtensive deformation, as proposed by Lodolo et al. (2003) and Esteban et al. (2014). However, in a geometrical model of rigid blocks, this fault bending may only explain around 10% of the slip rate difference.
3. The glaciation event, at its maximum thickness above the MFF in Chile while thinning towards the Atlantic coast, differently perturbed the tectonic activity along strike. Numerical models by Hampel et al. (2009) show that deformation in normal and reverse faults may be delayed beneath an ice cap and recovered when the ice melts. The same results may apply to strike-slip faults, because ice loading results in the flexure of the lithospheric plate which, in turn, increases the horizontal compressive stress in the seismogenic crust located in the inner arc of the flexed plate (Steffen & Steffen, 2021; Štěpančíková et al., 2022). For a vertical fault, it means an increase in stress orthogonal to the fault plane pushing away the system from rupture conditions. Consequently, during glaciation brittle deformation undergoes a delay that must be caught up after deglaciation. This deformation catch-up results in a higher average slip rate over the post-glacial period. The MFF would be the first example of strike-slip fault where this phenomenon is observed.

These results point out the need to study large strike-slip faults on several portions to unravel behaviour changes related to external or internal forcing. All slip rates along MFF are average values over the post-glacial period; their strike-along variation could be both spatial—if everywhere constant through time—and temporal. Studies on shorter time-scales are necessary to discriminate between these possibilities.

ACKNOWLEDGEMENTS

This work is part of Sandrine Roy Ph.D. thesis funded by the French Ministry of Higher Education and Research, CNRS-INSU-SYSTER programme and CNRS-IRD Défi Risques programme. Christian Sue acknowledges support from the CNRS-PICS project. We greatly thank LMC14 team for fruitful discussions about ^{14}C datings. We acknowledge Pablo Morales Vasquez, Ivette Martínez and Nativo Expediciones team for their essential support in fieldwork. We warmly thank Fabien Massot for his precious administrative support. We are grateful to P. Torres Carbonell and M. Rizza for their relevant suggestions that helped us to significantly improve the manuscript.

DATA AVAILABILITY STATEMENT

The data that support the findings of this study are available from the corresponding author upon reasonable request.

ORCID

Sandrine Roy  <https://orcid.org/0000-0003-3541-7765>

REFERENCES

- Arnold, M., Merchel, S., Boulès, D. L., Braucher, R., Benedetti, L., Finkel, R. C., Aumaître, G., Gottang, A., & Klein, M. (2010). The French accelerator mass spectrometry facility ASTER: Improved performance and developments. *Nuclear Instruments and Methods in Physics Research Section B: Beam Interactions with Materials and Atoms*, 268, 1954–1959. <https://doi.org/10.1016/j.nimb.2010.02.107>
- Bennett, R. A., Friedrich, A. M., & Furlong, K. P. (2004). Codependent histories of the San Andreas and San Jacinto fault zones from inversion of fault displacement rates. *Geology*, 32(11), 961–964.
- Bentley, M. J., Sugden, D. E., Hulton, N. R. J., & McCulloch, R. D. (2005). The landforms and pattern of deglaciation in the Strait of Magellan and Bahía Inútil, southernmost South America. *Geografiska Annaler: Series A, Physical Geography*, 87, 313–333. <https://doi.org/10.1111/j.0435-3676.2005.00261.x>
- Betka, P., Klepeis, K., & Mosher, S. (2016). Fault kinematics of the Magallanes–Fagnano fault system, southern Chile; An example of diffuse strain and sinistral transtension along a continental transform margin. *Journal of Structural Geology*, 85, 130–153. <https://doi.org/10.1016/j.jsg.2016.02.001>
- Boyd, B. L., Anderson, J. B., Wellner, J. S., & Fernandez, R. A. (2008). The sedimentary record of glacial retreat, Marinelli Fjord, Patagonia: Regional correlations and climate ties. *Marine Geology*, 255, 165–178.
- Bran, D. M., Palma, F., Menichetti, M., Lodolo, E., Bunicontró, S., Lozano, J. G., Baradello, L., Winocur, D., Grossi, M., & Tassone, A. A. (2023). Active faulting in the Beagle Channel (Tierra del Fuego). *Terra Nova*, 35, 1–14. <https://doi.org/10.1111/ter.12658>
- Braucher, R., Guillou, V., Boulès, D. L., Arnold, M., Aumaître, G., Keddadouche, K., & Nottoli, E. (2015). Preparation of ASTER in-house $^{10}\text{Be}/^{9}\text{Be}$ standard solutions. *Nuclear Instruments and Methods in Physics Research Section B: Beam Interactions with*

- Materials and Atoms*, 361, 335–340. <https://doi.org/10.1016/j.nimb.2015.06.012>
- Chevalier, M.-L., Van der Woerd, J., Tapponnier, P., Li, H., Ryerson, F. J., & Finkel, R. C. (2016). Late Quaternary slip-rate along the central Bangong-Chaxikang segment of the Karakorum fault, western Tibet. *GSA Bulletin*, 128(1–2), 284–314. <https://doi.org/10.1130/B31269.1>
- Clapperton, C. M., Sugden, D. E., Kaufman, D. S., & McCulloch, R. D. (1995). The last glaciation in central Magellan Strait, Southernmost Chile. *Quaternary Research*, 44, 133–148. <https://doi.org/10.1006/qres.1995.1058>
- Coronato, A., Meglioli, A., & Rabassa, J. (2004). Glaciations in the Magellan Straits and Tierra del Fuego, southernmost South America. In J. Ehlers, & P. L. Gibbard (Eds.), *Developments in quaternary sciences, Quaternary glaciations extent and chronology. PART III: South America, Asia, Africa, Australia and Antarctica* (Vol. 2, pp. 45–48). Elsevier.
- Coronato, A., Seppälä, M., Ponce, J. F., & Rabassa, J. (2009). Glacial geomorphology of the Pleistocene lake Fagnano ice lobe, Tierra del Fuego, southern South America. *Geomorphology*, 112, 67–81. <https://doi.org/10.1016/j.geomorph.2009.05.005>
- Costa, C. H., Smalley, R., Velasco, M. S., Schwartz, D. P., Ellis, M., & Ahumada, E. A. (2006). Paleoseismic observations of an onshore transform boundary: The Magallanes–Fagnano fault, Tierra del Fuego, Argentina. *Revista de la Asociación Geológica Argentina*, 61(4), 647–657.
- Cunningham, W. D. (1993). Strike-slip faults in the southernmost Andes and the development of the Patagonian orocline. *Tectonics*, 12, 169–186. <https://doi.org/10.1029/92TC01790>
- Davies, B. J., Darvill, C. M., Lovell, H., Bendle, J. M., Dowdeswell, J. A., Fabel, D., García, J.-L., Geiger, A., Glasser, N. F., Gheorghiu, D. M., Harrison, S., Hein, A. S., Kaplan, M. R., Martin, J. R. V., Mendelova, M., Palmer, A., Pelto, M., Rodés, Á., Sagredo, E. A., ... Thorndycraft, V. R. (2020). The evolution of the Patagonian ice sheet from 35 ka to the present day (PATICE). *Earth-Science Reviews*, 204, 103152. <https://doi.org/10.1016/j.earscirev.2020.103152>
- Dolan, J. F., McAuliffe, L. J., Rhodes, E. J., McGill, S. F., & Zinke, R. (2016). Extreme multi-millennial slip rate variations on the Garlock fault, California: Strain super-cycles, potentially time-variable fault strength, and implications for system-level earthquake occurrence. *Earth and Planetary Science Letters*, 446, 123–136. <https://doi.org/10.1016/j.epsl.2016.04.011>
- Dolan, J. F., van Dissen, R. J., Rhodes, E. J., Zinke, R., Hatem, A. E., McGuire, C., Langridge, R. M., & Grenader, J. R. (2024). One tune, many tempos: Faults trade off slip in time and space to accommodate relative plate motions. *Earth and Planetary Science Letters*, 625, 118484 ISSN 0012-821X.
- Dumoulin, J.-P., Comby-Zerbino, C., Delqué-Količ, E., Moreau, C., Caffy, I., Hain, S., Perron, M., Thellier, B., Setti, V., Berthier, B., & Beck, L. (2017). Status report on sample preparation protocols developed at the LMC14 Laboratory, Saclay, France: From sample collection to 14C AMS measurement. *Radiocarbon*, 59(3), 713–726. <https://doi.org/10.1017/RDC.2016.116>
- Esteban, F. D., Tassone, A., Lodolo, E., Menichetti, M., Lippai, H., Waldmann, N., Darbo, A., Baradello, L., & Vilas, J. F. (2014). Basement geometry and sediment thickness of Lago Fagnano (Tierra del Fuego). *Andean Geology*, 41, 293–313. <https://doi.org/10.5027/andgeoV41n2-a02>
- Febrer, J. M., Plasencia, M. P., & Sabbione, N. C. (2000). Local and regional seismicity from Ushuaia broadband station observations (Tierra del Fuego). *Terra Antartica*, 8, 35–40.
- Fernández, R., Gulick, S., Rodrigo, C., Domack, E., & Leventer, A. (2017). Seismic stratigraphy and glacial cycles in the inland passages of the Magallanes región of Chile, southernmost South America. *Marine Geology*, 386, 19–31. <https://doi.org/10.1016/j.margeo.2017.02.006>
- Ghiglione, M. C. (2002). Diques clásticos asociados a deformación trans-curren-te en depósitos sinorogénicos del Mioceno inferior de la Cuenca Austral. *Revista de la Asociación Geológica Argentina*, 57, 103–118.
- Gold, R. D., & Cowgill, E. (2011). Deriving fault-slip histories to test for secular variation in slip, with examples from the Kunlun and Awatere faults. *Earth and Planetary Science Letters*, 301, 52–64.
- Hall, B. L., Lowell, T. V., Bromley, G. R. M., Denton, G. H., & Putnam, A. E. (2019). Holocene glacier fluctuations on the northern flank of Cordillera Darwin, southernmost South America. *Quaternary Science Reviews*, 222, 105904. <https://doi.org/10.1016/j.quascirev.2019.105904>
- Hall, B. L., Porter, C. T., Denton, G. H., Lowell, T. V., & Bromley, G. R. (2013). Extensive recession of Cordillera Darwin glaciers in southernmost South America during Heinrich stadial 1. *Quaternary Science Reviews*, 62, 49–55. <https://doi.org/10.1016/j.quascirev.2012.11.026>
- Hampel, A., Hetzel, R., Maniatis, G., & Karow, T. (2009). Three-dimensional numerical modeling of slip rate variations on normal and thrust fault arrays during ice cap growth and melting. *Journal of Geophysical Research*, 114, B08406. <https://doi.org/10.1029/2008JB006113>
- Hogg, A. G., Hua, Q., Blackwell, P. G., Niu, M., Buck, C. E., Guilderson, T. P., Heaton, T. J., Palmer, J. G., Reimer, P. J., & Reimer, R. W. (2013). SHCal13 southern hemisphere calibration, 0–50,000 years cal BP. *Radiocarbon*, 55, 1889–1903. https://doi.org/10.2458/azu_js_rc.55.16783
- Jaschek, E. U., Sabbione, N. C., & Sierra, P. J. (1982). *Reubicación de sis-mos localizados en territorio Argentino, 1920–1963*. Observatorio Astronomico de la Universidad nacional de la Plata.
- Kirby, E., Harkins, N., Wang, E., Shi, X., Fan, C., & Burbank, D. (2007). Slip rate gradients along the eastern Kunlun fault. *Tectonics*, 26, TC2010. <https://doi.org/10.1029/2006TC002033>
- Klepeis, K. A. (1994). The Magallanes and Deseado fault zones: Major segments of the South American-Scotia transform plate boundary in southernmost South America, Tierra del Fuego. *Journal of Geophysical Research, Solid Earth*, 99, 22001–22014. <https://doi.org/10.1029/94JB01749>
- Klepeis, K. A., & Austin, J. A. (1997). Contrasting styles of superposed deformation in the southernmost Andes. *Tectonics*, 16, 755–776. <https://doi.org/10.1029/97TC01611>
- Lal, D. (1991). Cosmic ray labeling of erosion surfaces: In situ nuclide production rates and erosion models. *Earth and Planetary Science Letters*, 104, 424–439.
- Liu, J., Ren, Z., Zheng, W., Min, W., Li, Z., & Zheng, G. (2020). Late quaternary slip rate of the Aksay segment and its rapidly decreasing gradient along the Altyn Tagh fault. *Geosphere*, 16(6), 1538–1557. <https://doi.org/10.1130/GES02250.1>
- Lodolo, E., Menichetti, M., Bartole, B., Ben-Avraham, Z., Tassone, A., & Lippai, H. (2003). Magallanes–Fagnano continental transform fault (Tierra del Fuego, southernmost South America). *Tectonics*, 22, 15–26. <https://doi.org/10.1029/2003TC001500>
- Lomnitz, C. (1970). Major earthquakes and tsunamis in Chile during the period 1535 to 1955. *Geologische Rundschau*, 59, 938–960. <https://doi.org/10.1007/BF02042278>
- Matmon, A., Schwartz, D. P., Haeussler, P. J., Finkel, R., Lienkaemper, J. J., Stenner, H. D., & Dawson, T. E. (2006). Denali fault slip rates and Holocene–late Pleistocene kinematics of central Alaska. *Geology*, 34(8), 645–648.
- McCulloch, R. D., Fogwill, C. J., Sugden, D. E., Bentley, M. J., & Kubik, P. W. (2005). Chronology of the last glaciation in central Strait of Magellan and Bahía Inútil, southernmost South America. *Geografiska Annaler: Series A, Physical Geography*, 87, 289–312. <https://doi.org/10.1111/j.0435-3676.2005.00260.x>
- Mendoza, L., Richter, A., Fritsche, M., Hormaechea, J. L., Perdomo, R., & Dietrich, R. (2015). Block modeling of crustal deformation in Tierra

- del Fuego from GNSS velocities. *Tectonophysics*, 651–652, 58–65. <https://doi.org/10.1016/j.tecto.2015.03.013>
- Moreau, C., Messenger, C., Berthier, B., Hain, S., Thellier, B., Dumoulin, J.-P., Caffy, I., Sieudat, M., Delqué-Kolic, E., Mussard, S., Perron, M., Setti, V., & Beck, L. (2020). Artemis, the 14C AMS Facility of the LMC14 National Laboratory: A status report on quality control and microsample procedures. *Radiocarbon*, 62(6), 1755–1770. <https://doi.org/10.1017/RDC.2020.73>
- Ninis, D., Little, T. A., Dissen, R. J. V., Litchfield, N. J., Smith, E. G. C., Wang, N., Rieser, U., & Henderson, C. M. (2013). Slip rate on the Wellington fault, New Zealand, during the late quaternary: Evidence for variable slip during the Holocene. *Bulletin of the Seismological Society of America*, 103(1), 559–579. <https://doi.org/10.1785/0120120162>
- Onorato, M. R., Perucca, L. P., Coronato, A., Prezzi, C., Blanc, P. A., Lopez, R., & Magneres, I. (2021). Morphotectonic characterization along the eastern portion of the main trace of Magallanes–Fagnano Fault System in Tierra del Fuego, Argentina. *Journal of South American Earth Sciences*, 112, 103550. <https://doi.org/10.1016/j.jsames.2021.103550>
- Pankhurst, R. J. (2000). Episodic silicic volcanism in Patagonia and the Antarctic Peninsula: Chronology of magmatism associated with the break-up of Gondwana. *Journal of Petrology*, 41, 605–625. <https://doi.org/10.1093/petrology/41.5.605>
- Pelayo, A. M., & Wiens, D. A. (1989). Seismotectonics and relative plate motions in the Scotia Sea region. *Journal of Geophysical Research*, 94(B6), 7293–7320. <https://doi.org/10.1029/JB094iB06p07293>
- Perucca, L., Alvarado, P., & Saez, M. (2016). Neotectonics and seismicity in southern Patagonia. *Geological Journal*, 51, 545–559. [https://doi.org/10.1016/S1571-0866\(07\)10005-1](https://doi.org/10.1016/S1571-0866(07)10005-1)
- Rabassa, J., Coronato, A., Bujalesky, G., Saleme, M., Roig, C., Meglioli, A., Heusser, C., Gordillo, S., Roig, F., Borromei, A., & Quattrocchio, M. (2000). Quaternary of Tierra del Fuego, southernmost South America: An updated review. *Quaternary International*, 68–71, 217–240. [https://doi.org/10.1016/S1040-6182\(00\)00046-X](https://doi.org/10.1016/S1040-6182(00)00046-X)
- Ramsey, C. B. (2009). Bayesian analysis of radiocarbon dates. *Radiocarbon*, 51, 337–360. <https://doi.org/10.1017/S0033822200033865>
- Ramsey, C. B. (2017). Methods for summarizing radiocarbon datasets. *Radiocarbon*, 59, 1809–1833. <https://doi.org/10.1017/RDC.2017.108>
- Reynhout, S. A., Kaplan, M. R., Sagredo, E. A., Aravena, J. C., Soteres, R. L., Schwartz, R., & Schaefer, J. M. (2021). Holocene glacier history of northeastern Cordillera Darwin, southernmost South America (55°S). *Quaternary Research*, 105, 166–181. <https://doi.org/10.1017/qua.2021.45>
- Roy, S., Vassallo, R., Martinod, J., Ghiglione, M. C., Sue, C., & Allemand, P. (2020). Co-seismic deformation and post-glacial slip rate along the Magallanes–Fagnano fault, Tierra Del Fuego, Argentina. *Terra Nova*, 32, 1–10. <https://doi.org/10.1111/ter.12430>
- Sandoval, F. B., & de Pascale, G. P. (2020). Slip rates along the narrow Magallanes fault system, Tierra del Fuego region, Patagonia. *Scientific Reports*, 10, 1–13. <https://doi.org/10.1038/s41598-020-64750-6>
- Smalley, R., Kendrick, E., Bevis, M. G., Dalziel, I. W. D., Taylor, F., Lauría, E., & Piana, E. (2003). Geodetic determination of relative plate motion and crustal deformation across the Scotia–South America plate boundary in eastern Tierra del Fuego. *Geochemistry, Geophysics, Geosystems*, 4, 1070. <https://doi.org/10.1029/2002GC000446>
- Steffen, R., & Steffen, H. (2021). Reactivation of non-optimally orientated faults due to glacially induced stresses. *Tectonics*, 40, e2021TC006853. <https://doi.org/10.1029/2021TC006853>
- Štěpančíková, P., Rockwell, T. K., Stemberk, J., Rhodes, E. J., Hartvich, F., Luttrell, K., Myers, M., Tábořík, P., Rood, D. H., Wechsler, N., Nývt, D., Ortuno, M., & Hók, J. (2022). Acceleration of Late Pleistocene activity of a Central European fault driven by ice loading. *Earth and Planetary Science Letters*, 591, 117596. <https://doi.org/10.1016/j.epsl.2022.117596>
- Stone, J. O. (2000). Air pressure and cosmogenic isotope production. *Journal of Geophysical Research: Solid Earth*, 105, 23753–23759. <https://doi.org/10.1029/2000JB900181>
- Tassone, A., Lippai, H., Lodolo, E., Menichetti, M., Comba, A., Hormaechea, J. L., & Vilas, J. F. (2005). A geological and geophysical crustal section across the Magallanes–Fagnano fault in Tierra del Fuego. *Journal of South American Earth Sciences*, 19, 99–109. <https://doi.org/10.1016/j.jsames.2004.12.003>
- Tassone, A., Lodolo, E., Menichetti, M., Yagupsky, D. L., Caffau, M., & Vilas, J. F. A. (2008). Seismostratigraphic and structural setting of the Malvinas Basin and its southern margin (Tierra del Fuego Atlantic offshore). *Geologica Acta*, 6, 55–67.
- Thomas, C. R. (1949). Geology and petroleum exploration in Magallanes Province, Chile. *AAPG Bulletin*, 33, 1553–1578. <https://doi.org/10.1306/3D933DEE-16B1-11D7-8645000102C1865D>
- Torres Carbonell, P. J., Dimieri, L. V., Olivero, E. B., Bohoyo, F., & Galindo-Zaldívar, J. (2014). Structure and tectonic evolution of the Fuegian Andes (southernmost South America) in the framework of the Scotia Arc development. *Global and Planetary Change*, 123, 174–188. <https://doi.org/10.1016/j.gloplacha.2014.07.019>
- Torres Carbonell, P. J., Olivero, E. B., & Dimieri, L. V. (2008). Control en la magnitud de desplazamiento de rumbo del Sistema Transformante Fagnano, Tierra del Fuego, Argentina. *Revista Geologica de Chile*, 35, 63–77. <https://doi.org/10.5027/andgeoV35n1-a03>
- Winslow, M. A. (1982). The structural evolution of the Magallanes Basin and neotectonics in the southernmost Andes. *Antarctic Geoscience*, 4, 143–154.
- Zinke, R., Dolan, J. F., Rhodes, E. J., van Dissen, R. J., Hatem, A. E., McGuire, C. P., Brown, N. A., & Grenader, J. R. (2021). Latest Pleistocene–Holocene incremental slip rates of the Wairau fault: Implications for long-distance and long-term coordination of faulting between North and South Island, New Zealand. *Geochemistry, Geophysics, Geosystems*, 22(9), e2021GC009656. <https://doi.org/10.1029/2021GC009656>

SUPPORTING INFORMATION

Additional supporting information can be found online in the Supporting Information section at the end of this article.

Data S1.

How to cite this article: Vassallo, R., Martinod, J., Roy, S., Sue, C., & Astrade, L. (2024). Along-strike variation of fault slip rate of a transform plate boundary in Tierra del Fuego (South Patagonia). *Terra Nova*, 00, 1–9. <https://doi.org/10.1111/ter.12715>